

Stability of quantitative evaluation method of liver fibrosis using amplitude distribution model of fibrotic liver

病変肝の振幅分布モデルを用いた肝病変定量評価手法の安定性の検討

Yu Igarashi^{1‡}, Tadashi Yamaguchi² and Hiroyuki Hachiya¹ (¹Tokyo Inst. of Tech.; ²Chiba Univ.)

五十嵐悠^{1‡}, 山口匡², 蜂屋弘之¹ (¹東工大; ²千葉大)

1. Introduction

In order to realize quantitative diagnosis of liver fibrosis, we have been analyzing the probability density function (PDF) of echo amplitude using B-mode images¹⁻³. To achieve the quantitative diagnosis of the stage of liver fibrosis, we proposed an amplitude distribution model using two Rayleigh distributions⁴. We have been studying possibility of the quantitative estimation of liver fibrosis by using the model. In this paper, we present the stability of the quantitative evaluation method of liver fibrosis using the amplitude distribution model by the simulation, and compare the results using the simulation and clinical data.

2. Amplitude distribution model of liver fibrosis

When scattered points are distributed closely and uniformly, such as the normal liver tissue, interference-induced random fluctuation in brightness in the image called speckle pattern appears. The PDF of echo envelope of speckle pattern can be approximated by Rayleigh distribution. On the other hand, in inhomogeneous medium, such as the liver fibrosis, the PDF of echo envelopes deviates from Rayleigh distribution. It is thought that fibrotic liver is composed of normal liver and fibrosis tissues. We proposed the amplitude distribution model for liver fibrosis in which the distribution is modeled by combination of Rayleigh distributions with low variance σ_{low}^2 (normal liver) and high variance σ_{high}^2 (fibrosis tissues).

Rayleigh distribution is given by

$$p(x) = \frac{x}{\sigma^2} \exp\left(-\frac{x^2}{2\sigma^2}\right), \tag{1}$$

where x, σ^2 is the echo amplitude and the variance of the echo amplitude, respectively.

Amplitude distribution model of liver fibrosis is given by

$$p_{mix}(x) = (1-\alpha)p_{low}(x) + \alpha p_{high}(x) \tag{2}$$

where $p_{high}(x)$ is Rayleigh distribution with high

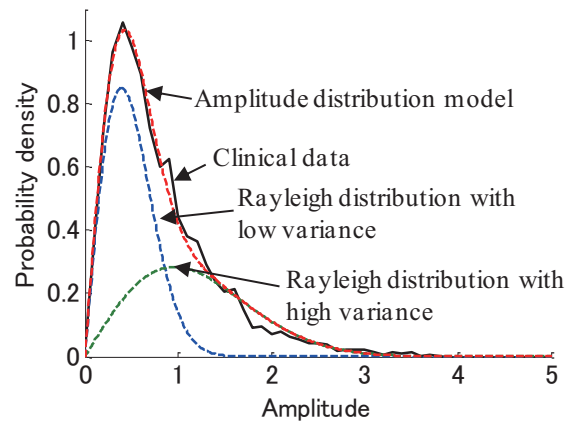


Fig. 1 Combination of two Rayleigh distributions.

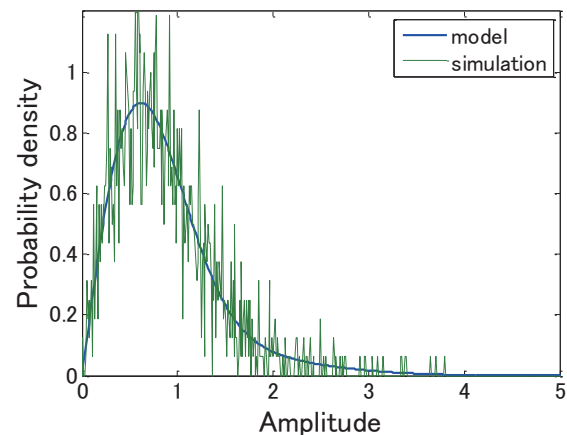


Fig. 2 PDF calculated the simulation based on amplitude distribution model of liver fibrosis.

variance, $p_{low}(x)$ is Rayleigh distribution with low variance and α ($0 \leq \alpha \leq 1$) is the mixture rate of Rayleigh distribution with high variance. Therefore, model parameters (indices of fibrillization) are the variance ratio ($\sigma_{high}^2 / \sigma_{low}^2$) and the mixture rate (α).

Variance ratio and mixture rate are related to the fibrosis stage and the amount of fibrous tissues respectively. **Figure 1** shows an example of the combination of two Rayleigh distributions.

In order to decide model parameters in clinical echo data, we used skewness ($E[(x-u_x)^3] / \sigma_x^3$) and kurtosis ($E[(x-u_x)^4] / \sigma_x^4 - 3$)

E-mail address: igarashi.y.aa@m.titech.ac.jp

calculated from the PDF. u_x, σ_x are the mean and standard deviation of x . We calculated model parameters from these parameters as an inverse problem. The PDF with model parameters [1, 0%] (= [the variance ratio, the mixture rate]) is Rayleigh distribution (normal liver). If model parameters increase, the PDF deviates from Rayleigh distribution (that is, liver fibrosis proceeds).

3. Stability of model parameters estimation

We estimated the statistical stability of the inversion problem of model parameters based on the amplitude distribution model. In this simulation, an amplitude histogram was generated from Rayleigh distributed random variables as shown in **Figure 2**. The number of random variables in one trial of the simulation is 1600 because a ROI size of clinical data is 40×40 pixel (about 4.2 mm in depth × 8.4mm in the lateral direction).

Figure 3(a) (b) shows polar plot of fibrosis evaluation of clinical echo data. The radius and the phase parameters correspond to the variance ratio and the mixture rate. Clinical echo data sets (*in vivo*) of liver fibrosis are classified by New-Inuyama classification using the result of biopsy. There is little difference between the mixture rates of normal and cirrhosis liver cases. The variance ratio converges on 1 in case of a normal liver, and the variance ratio increases in case of cirrhosis.

We evaluated the degree of the fibrillization by using the polar plot of the simulation to examine the stability of quantitative evaluation method. The polar plots that correspond to a normal liver and cirrhosis are shown in **Figure 4(a) (b)**. The number of random variables in one trial on Fig. 4 is 1600. The number of trials of the simulation is 2000. The same tendency can be seen on a normal liver case compared with Fig. 3 obtained from clinical data. In case of cirrhosis, it can be seen that clinical data results has larger variation compared with the simulation results. It means that large difference of mixture rate (fibrotic tissue amount) is caused by not only statistical fluctuation but also tissue acoustic structure variation.

4. Conclusion

We examined stability of quantitative evaluation of liver fibrosis using amplitude distribution model of fibrotic liver by the simulation, and compared the results using the simulation and clinical echo data. In the case of normal liver, it is confirmed that estimated results from clinical echo data are similar to results using the simulation. When the stage of liver fibrosis proceeds, it is confirmed that the statistical fluctuation on the simulation results is smaller than the variation on

clinical data results. Large difference of fibrotic tissue amount is caused by not only statistical fluctuation but also tissue acoustic structure variation.

We will examine a robust quantitative evaluation method using clinical echo data at various stages.

Acknowledgment

This work was partially supported by Grant-in-Aid for Scientific Research and the Research and Development Committee Program of JSUM.

References

1. T.Yamaguchi, H.Hachiya: Jpn. J. Appl. Phys. **37** (1998) 3093.
2. H. Yamada, *et.al.*: J. Hepatology **44** (2006) 68.
3. T. Yamaguchi, *et al.*: J Med Ultrasonics, DOI10.1007/s10396-010-0270-y (2010).
4. Y. Igarashi, *et al.*: Jpn. J. Appl. Phys. **49** (2010) 07HF06.

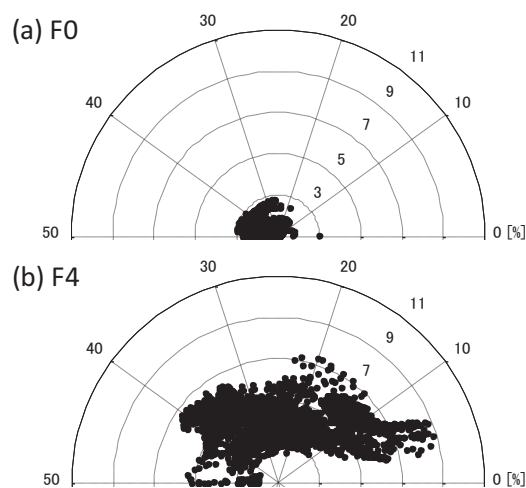


Fig. 3 Polar plot of fibrosis evaluation of clinical data. (a)normal liver, (b)cirrhotic liver.

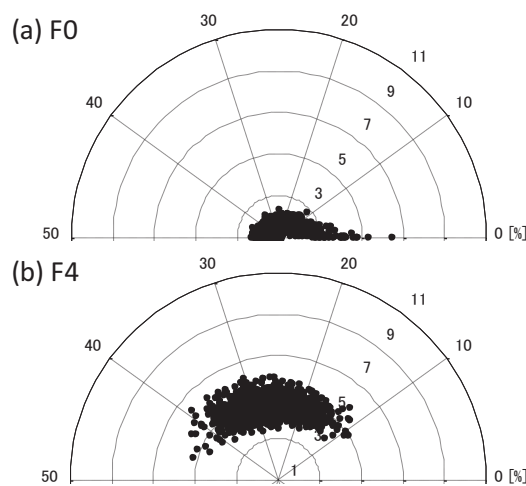


Fig. 4 Polar plot of fibrosis evaluation calculated from simulated PDF. (a)normal liver, (b)cirrhotic liver